Video Article

# Facile Preparation of Ultrafine Aluminum Hydroxide Particles with or without Mesoporous MCM-41 in Ambient Environments

Viktor Dubovoy[1], Ravi Subramanyam[1], Michael Stranick[1], Laurence Du-Thumm[1], Long Pan[1]

[1]Colgate-Palmolive Company

Correspondence to: Long Pan at Long_Pan@colpal.com

URL: https://www.jove.com/video/55423
DOI: doi:10.3791/55423

Keywords: Chemistry, Issue 123, hydrolysis, aluminum hydroxide, nanogibbsite, mesoporous silica, $^{27}$Al nuclear magnetic resonance, size-exclusion chromatography, hydrodynamic radius

Date Published: 5/11/2017

Citation: Dubovoy, V., Subramanyam, R., Stranick, M., Du-Thumm, L., Pan, L. Facile Preparation of Ultrafine Aluminum Hydroxide Particles with or without Mesoporous MCM-41 in Ambient Environments. *J. Vis. Exp.* (123), e55423, doi:10.3791/55423 (2017).

## Abstract

An aqueous suspension of nanogibbsite was synthesized via the titration of aluminum aqua acid $[Al(H_2O)_6]^{3+}$ with L-arginine to pH 4.6. Since the hydrolysis of aqueous aluminum salts is known to produce a wide array of products with a wide range of size distributions, a variety of state-of-the-art instruments (*i.e.,* $^{27}$Al/$^{1}$H NMR, FTIR, ICP-OES, TEM-EDX, XPS, XRD, and BET) were used to characterize the synthesis products and identification of byproducts. The product, which was comprised of nanoparticles (10-30 nm), was isolated using gel permeation chromatography (GPC) column technique. Fourier transform infrared (FTIR) spectroscopy and powder X-ray diffraction (PXRD) identified the purified material as the gibbsite polymorph of aluminum hydroxide. The addition of inorganic salts (*e.g.*, NaCl) induced electrostatic destabilization of the suspension, thereby agglomerating the nanoparticles to yield $Al(OH)_3$ precipitate with large particle sizes. By utilizing the novel synthetic method described here, $Al(OH)_3$ was partially loaded inside the highly ordered mesoporous framework of MCM-41, with average pore dimensions of 2.7 nm, producing an aluminosilicate material with both octahedral and tetrahedral Al ($O_h/T_d$ = 1.4). The total Al content, measured using energy-dispersive X-ray spectrometry (EDX), was 11% w/w with a Si/Al molar ratio of 2.9. A comparison of bulk EDX with surface X-ray photoelectron spectroscopy (XPS) elemental analysis provided insight into the distribution of Al within the aluminosilicate material. Furthermore, a higher ratio of Si/Al was observed on the external surface (3.6) as compared to the bulk (2.9). Approximations of O/Al ratios suggest a higher concentration of $Al(O)_3$ and $Al(O)_4$ groups near the core and external surface, respectively. The newly developed synthesis of Al-MCM-41 yields a relatively high Al content while maintaining the integrity of the ordered silica framework and can be used for applications where hydrated or anhydrous $Al_2O_3$ nanoparticles are advantageous.

## Video Link

The video component of this article can be found at https://www.jove.com/video/55423/

## Introduction

Materials made of aluminum hydroxide are promising candidates for a variety of industrial applications, including catalysis, pharmaceuticals, water treatment, and cosmetics.[1,2,3,4] At elevated temperatures, aluminum hydroxide absorbs a substantial amount of heat during decomposition to yield alumina ($Al_2O_3$), making it a useful flame-retarding agent.[5] The four known polymorphs of aluminum hydroxide (*i.e.*, gibbsite, bayerite, nordstrandite, and doyleite) have been investigated using computational and experimental techniques to improve our understanding of the formation and structures thereof[6]. The preparation of nanoscale particles is of particular interest due to their potential to exhibit quantum effects and properties differing from those of their bulk counterparts. Nanogibbsite particles with dimensions on the order of 100 nm are easily prepared under various conditions[7,8,9,10,11,12,13,14].

Overcoming inherent challenges associated with reducing the particle sizes further is difficult; therefore, only a few cases exist where nanogibbsite particles have dimensions on the order of 50 nm.[14,15,16,17] To the best of our knowledge, there have been no reports of nanogibbsite particles smaller than 50 nm. In part, this is attributed to the fact that nanoparticles tend to agglomerate due to electrostatic instability and the high probability for the formation of hydrogen bonds between the colloidal particles, especially in polar protic solvents. Our objective was to synthesize small $Al(OH)_3$ nanoparticles by using exclusively safe ingredients and precursors. In the current work, aqueous particle aggregation was inhibited by incorporating an amino acid (*i.e.*, L-arginine) as a buffer and stabilizer. Moreover, it is reported that the guanidinium-containing arginine prevented aluminum hydroxide particle growth and aggregation to yield an aqueous colloidal suspension with average particle sizes of 10-30 nm. It is proposed here that the amphoteric and zwitterionic properties of arginine mitigated the surface charge of aluminum hydroxide nanoparticles during the mild hydrolysis to disfavor particle growth beyond 30 nm. Although arginine was not capable of reducing the particle size below 10 nm, such particles were achieved by taking advantage of the "cage" confinement effect within the mesopores of MCM-41. Characterization of the Al-MCM-41 composite material revealed ultrafine aluminum hydroxide nanoparticles within the mesoporous silica, which has an average pore size of 2.7 nm.

## Protocol

## 1. $Al(OH)_3$ Nanoparticle Synthesis

1. Dissolve 1.40 g of aluminum chloride hexahydrate in 5.822 g of deionized water.
2. Add 2.778 g of L-arginine to the aqueous aluminum chloride solution while under magnetic stirring. Add the L-arginine slowly, so that the added arginine dissolves and does not form large clumps or chunks; furthermore, a slow addition reduces local concentrations of alkalinity and provides conditions for a more controllable hydrolysis.
3. Once all the arginine dissolves into the solution, heat the solution for 72 h at 50 °C; at this point, the solution may appear as a cloudy suspension.

## 2. Precipitating $Al(OH)_3$ with NaCl

1. Prepare a GPC column that is 49 in long and 1.125 in diameter. Pack the gel in successive steps of adding gel and allowing water to flow through the column to ensure proper packing, with minimal space between the gel beads. Pack the gel to about 80% of the column; the amount of gel packed varies every time and only affects the retention time of the separated species.
2. Introduce 10 mL of as-synthesized $Al(OH)_3$ nanoparticle suspension (prepared in step 1.3) into the column using an HPLC pump with a 10 mL injector loop. Custom-make the injector loop using tubing with an external diameter of approximately 0.125 in and a length that is calibrated to deliver 10 mL of injected sample.
3. **Collect the column elution in intervals correlating with the dRI peak location. Connect the GPC output to the input of a differential refractive index (dRI) detector.**
   NOTE: As separated species come out of the GPC, they appear on the dRI detector as a peak and are then collected in 125 mL bottles. The GPC column produces two well-resolved peaks, which are both collected and analyzed with size-exclusion chromatography (SEC) and elemental analysis (EA) to discern arginine from aluminum species. The total volume collected will depend on size of the GPC column, the total amount of packing material used, and the flow rate of the deionized water used to elute the column.
   1. Collect the majority of the peak 1 fraction over 100 min at a 0.2 mL/min flow rate.
   2. Collect the eluent in 30 min intervals once a peak emerges on the RI detector of the GPC column.
      NOTE: Changing the interval range will change the concentration and purity of the resulting purified peak 1 material. It is better to collect small intervals of the peak at first to determine which portion contains the highest concentration and purity of peak 1 species for a specific column.
4. Prepare 1 wt% of NaCl.
5. Add the prepared NaCl solution dropwise to 10 mL of purified $Al(OH)_3$ nanoparticles; the material prepared using NaCl precipitation is not used for further experiments.

## 3. Preparation of Al-MCM-41

1. Activate approximately 1.0 g of MCM-41 at 120 °C under vacuum for 3 h in a vacuum oven.
2. Prepare 50.0 g of aluminum chloride solution by combining 9.6926 g of $AlCl_3 \cdot 6H_2O$ with 40.3074 g of deionized water.
3. Add 0.7 g of activated MCM-41 to 50.0 g of aluminum chloride solution (prepared in step 3.2).
4. Allow adequate mixing time (1 h) to ensure homogeneity of the $AlCl_3$ diffused throughout the MCM-41 channels.
5. Add L-arginine to the heterogeneous mixture to an Arg/Al molar ratio of 2.75 under magnetic stirring. Similarly to step 1.2, add the arginine slowly enough so as to allow the instantaneously formed flocculates to redissolve and reduce the clumping of the arginine before continuing the addition.
6. Once homogeneous, heat the mixture at 50 °C for 72 h.
7. Filter the obtained heterogeneous solution using a Buchner funnel, under vacuum and equipped with qualitative 90 mm filter paper circles (or any other appropriate filter papers).
8. Wash the filtered white powder with excess deionized water to ensure the removal of unreacted aluminum chloride, arginine, or water-soluble byproducts from the produced Al-MCM-41 material.

## Representative Results

### Nanogibbsite Synthesis

Nanogibbsite was prepared by titrating $AlCl_3 \cdot 6H_2O$ (14 wt%) with L-arginine to a final Arg/Al molar ratio of 2.75. The synthesis of nanogibbsite particles was monitored via *SEC,* which is a widely used analysis technique for partially hydrolyzed aluminum chloride solutions, capable of discerning five domains arbitrarily designated as peaks 1, 2, 3, 4, and 5[1]. Here, we report that nanogibbsite particles with particle sizes of 10-30 nm are components of various potential structures that elute under the peak 1 domain of typical SEC analysis. To the best of our knowledge, the identification of molecules that elute within SEC peak 1 has not been described in the literature thus far. Powder X-ray diffraction (PXRD) and Fourier transform infrared spectroscopy (FTIR) experiments were able to unambiguously identify the $Al(OH)_3$ structure. Elution from the GPC column yielded a translucent $Al(OH)_3$ suspension with 99% purity (based on Al content), a pH of 6.7, +8.9 mV zeta potential (electrophoretic mobility and conductivity of 0.7 µm·cm/V·s and 0.7 mS/cm, respectively), and undetectable amounts of nitrogen. Non-stoichiometric amounts of chloride (Al:Cl ratio of 35:1) anions were detected after purification with GPC, which suggests the presence of partially hydrolyzed cationic impurities with the stoichiometry $[Al(OH)_xCl_{3-x}]$ (where x is the molar hydrolysis ratio typically in the range of 0-3), which are likely responsible for the positive zeta potential. The powder obtained by freeze-drying the purified solution was not soluble in water. The oxygen to aluminum ratio (3.3:1) was in good agreement with $Al(OH)_3$ stoichiometry. SEC analysis indicates that the nanogibbsite particles can be synthesized at a conversion rate of 82%. Subsequent characterization was conducted on the GPC-purified material.

### Characterization

FTIR analysis confirmed the gibbsite polymorph structure by the presence of a characteristic OH stretch at 3,620 $cm^{-1}$, which can be discerned from that of bayerite (3,650 $cm^{-1}$)[2,3]. Furthermore, other gibbsite vibration modes were evident from the absorptions at 3,617, 3,523, 3,453, 1,023, 970, and 918 $cm^{-1}$ [4,5,6]. Arginine was not detected by the FTIR method. Static light scattering analysis of the sample with an Arg/Al molar ratio of 2.75 indicated that the average particle size was in the range of 10-30 nm. The calculated crystallite size, calculated from the XRD pattern using the Scherrer equation[7,8], was ~8 nm, which is in decent agreement with light scattering data. Discrete particles with diameters in the range of 5-15 nm were observed in TEM images (**Figure 1**).

$^{27}Al$ NMR was measured for samples with Arg/Al molar ratios of 0, 2.25, and 2.75 (**Figure 2**). The results indicate that Al monomer (*i.e.*, $AlCl_3$), which has a characteristic sharp signal at 0 ppm, hydrolyzed to yield Keggin clusters (*i.e.*, $Al_{13\text{-}mer}$ and $Al_{30\text{-}mer}$) at an Arg/Al ratio of 2.25, as evidenced by their characteristic 63- and 70-ppm signals. The maximum concentration of Keggin clusters was measured at an Arg/Al of 2.25, which is in good agreement with the SEC data. At an Arg/Al ratio of 2.75, the $^{27}Al$ NMR spectra exhibited a single $O_h$ signal at 8 ppm.

### Al-MCM-41 Synthesis and Characterization

Since its discovery in 1992, MCM-41 has been of great scientific and industrial interest for various applications, such as catalysis, drug delivery, and separations. Unlike zeolites, the structure of MCM-41-type materials can be tailored to exhibit uniform pore sizes between 1.6-10 nm in diameter and generally have surface areas on the order of 1,000 $m^2g^{-1}$. Here, MCM-41, with an average pore size of 2.7 nm, was used as a support "cage" for the confined growth of nanogibbsite particles. Prior to Al loading, MCM-41 was activated at 120 °C to remove any adsorbed contaminants (*e.g.*, water, atmospheric gasses, *etc.*) from the silica surface. Subsequently, aluminum chloride solution was added to the purely siliceous MCM-41 solid and allowed to equilibrate with $Al^{3+}$ adsorption within the pores of MCM-41 for 1 h. The slow addition of arginine powder under magnetic stirring caused local flocculation, which was allowed to dissipate prior to further arginine addition. Product formation in the bulk solution was monitored using SEC analysis and $^{27}Al$ NMR, which indicated that the aluminum chloride was effectively converted into predominantly peak 1 and nanogibbsite species, respectively. The resulting Al-MCM-41 material was filtered and washed with copious amounts of water prior to characterization.

The $^{27}Al$ MAS NMR (**Figure 3**) of the prepared Al-MCM-41 material demonstrates the presence of both octahedral (~2 ppm) and tetrahedral (~57 ppm) Al environments, which are commonly observed in mesoporous silica modified with Al species[12]. The $O_h/T_d$ ratio was measured at 1.4. The bulk (EDX) elemental composition was 8.02% Al, 23.26% Si, and 68.70% O. The surface (XPS) elemental composition consisted of 6.13% Al, 21.75% Si, and 66.36% O, which suggests that there is a smaller content of Al on the surface of the particles as compared to the bulk counterpart. The Si/Al ratio was 2.9 and 3.6, as measured by EDX and XPS, respectively. The higher ratio of Si/Al observed in XPS versus EDX analysis indicates that a larger fraction of Al penetrated into the pores as opposed to building up on the surface. Chloride was not detected in stoichiometric concentrations using either method.

Small-angle X-ray diffraction (SAXRD) patterns were measured before and after Al loading and were indexed based on hexagonal symmetry (**Figure 4**). The presence of 100 (2.2°), 110 (3.9°), 200 (4.4°), and 210 (5.8°) lattice reflections were observed in both samples, indicating that significant changes in the highly ordered porosity did not occur as a result of Al insertion. Brunauer-Emmett-Teller (BET) analysis of the original MCM-41 material yielded a BET surface area of 997 $m^2/g$, a pore volume of 0.932 $cm^3/g$, and a pore width of 2.7 nm. BET data after grafting Al demonstrated a BET surface area of 742 $m^2/g$ (20.4% reduction), a pore volume of 0.649 $cm^3/g$ (30.4% reduction), and a pore width of 2.1 nm (22.2% reduction). Moreover, the incorporation of Al within the pores reduced the overall $N_2$ adsorbed from 602 to 419 cc/g. The $N_2$ desorption curve (not shown) exhibited a hysteresis loop typical of uniform mesoporosity. $^1H$ MAS NMR was also measured before and after Al particle growth within the mesopores. The introduction of Al caused a downfield shift (~1 ppm) for the predominant 3.1-ppm signal observed in MCM-41. A new, isolated signal emerged at 0.9 ppm, which was assigned to hydroxyl protons coordinating with aluminum atoms, since it experiences relatively stronger shielding and is commonly observed in acidic zeolite materials made of aluminum[15,16,17].

$^{27}Al$ nuclear magnetic resonance ($^{27}Al$ NMR) and pH measurements were obtained for samples with varied Arg/Al ratios (**Figures 2** and **5**). FTIR-ATR and transmission electron microscope (TEM) experiments were conducted for nanogibbsite prepared with an Arg/Al molar ratio of 2.75 (**Figures 1** and **6**). After loading Al into MCM-41 void space, $^{27}Al$ MAS NMR, $N_2$ adsorption, SAXRD, $^1H$ MAS NMR, and TEM analyses were carried out to characterize the prepared Al-MCM-41 material (**Figures 3, 4,** and **7-10**).

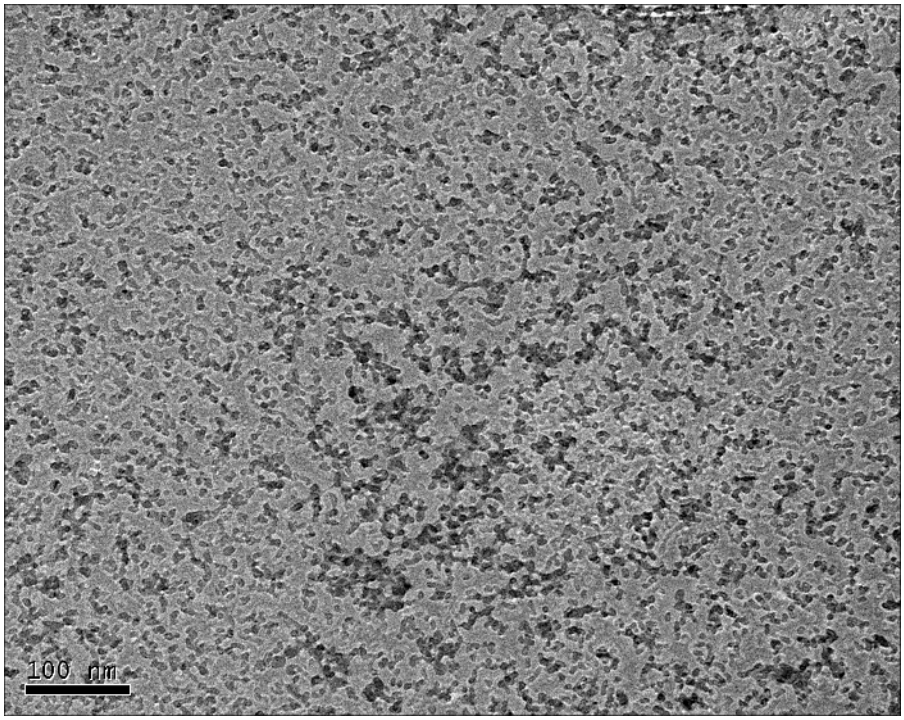


**Figure 1:** TEM micrograph of purified nano-Al(OH)$_3$ with a scale bar of 100 nm. Please click here to view a larger version of this figure.

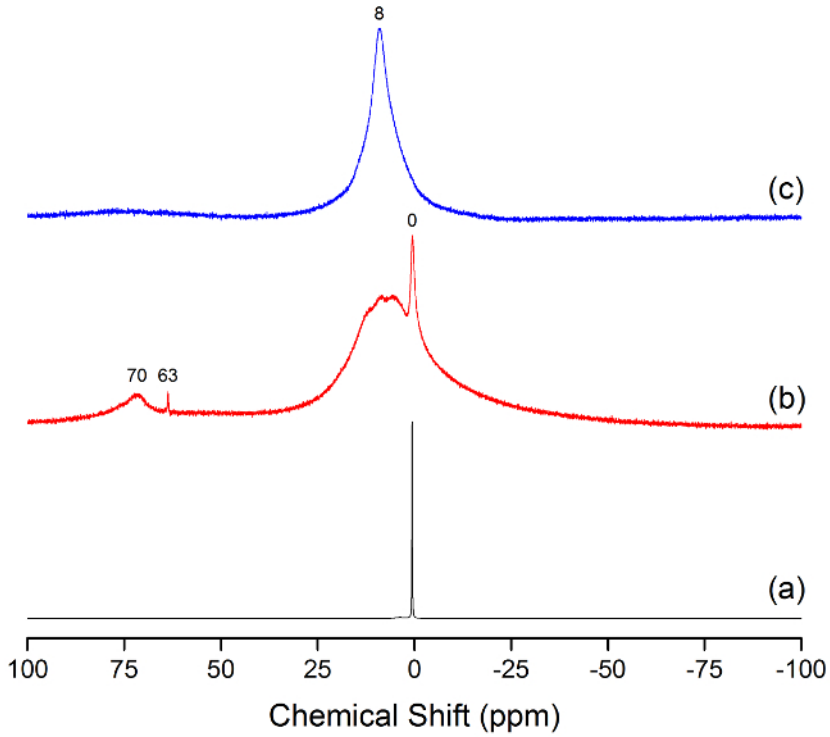


**Figure 2:** Liquid $^{27}$Al NMR of samples with Arg/Al rations of 0 (**a**), 2.25 (**b**), and 2.75 (**c**). The main peaks at 0, 8, 63, and 70 ppm are noted above the respective peak positions. Please click here to view a larger version of this figure.

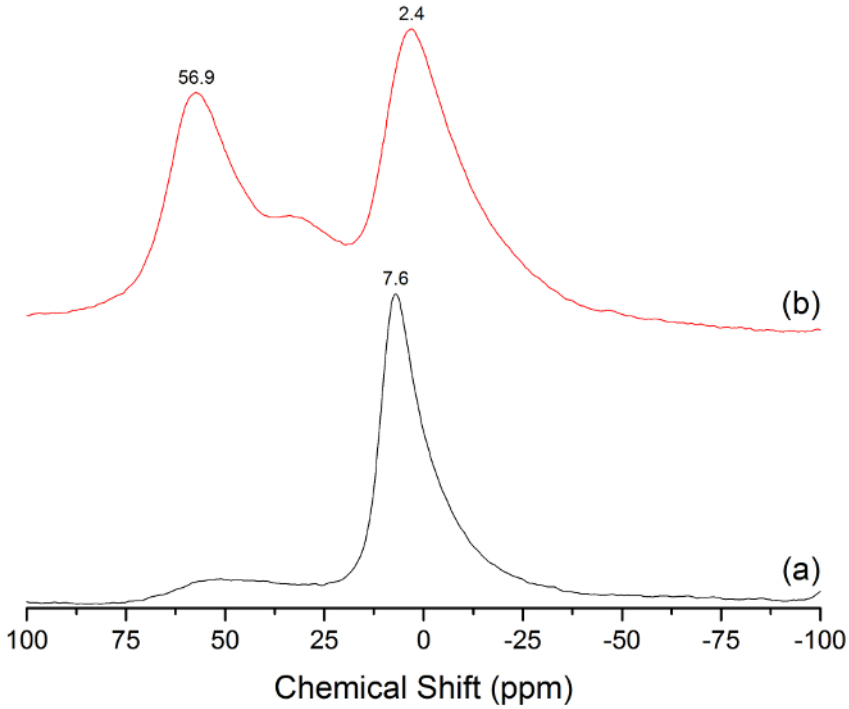


**Figure 3:** $^{27}$Al MAS NMR spectrum of prepared nanogibbsite (**a**) and prepared Al-MCM-41 (**b**). The major peaks at 7.6, 2.4, and 56.9 ppm are labeled above the respective peak positions. Please click here to view a larger version of this figure.

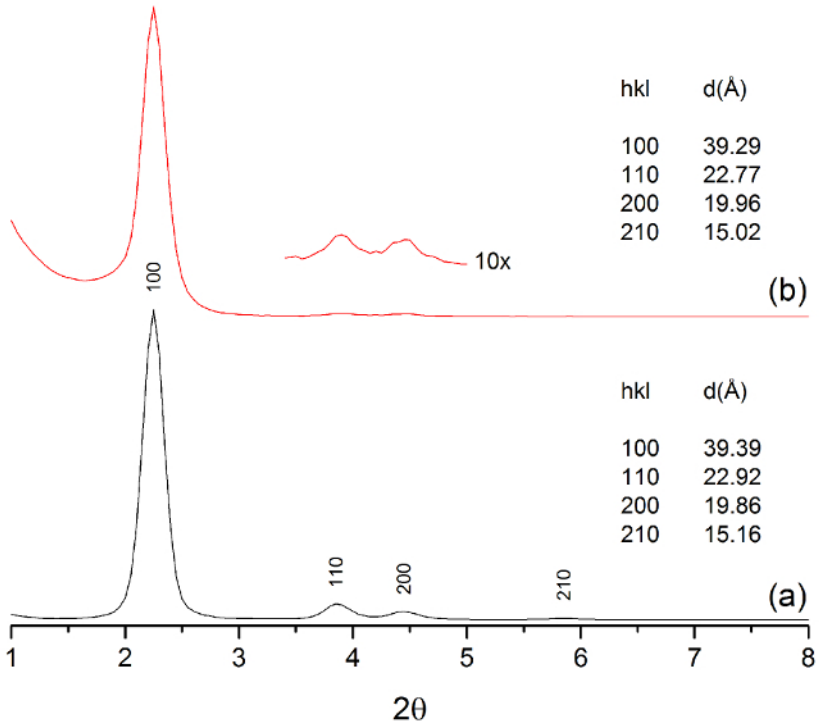


**Figure 4:** SAXRD diffraction pattern of MCM-41 (**a**) and Al-MCM-41 (**b**), with their tabulated lattice reflections and corresponding d-spacing. The 110 and 200 reflections are magnified 10X in the Al-MCM-41 diffraction pattern. Please click here to view a larger version of this figure.

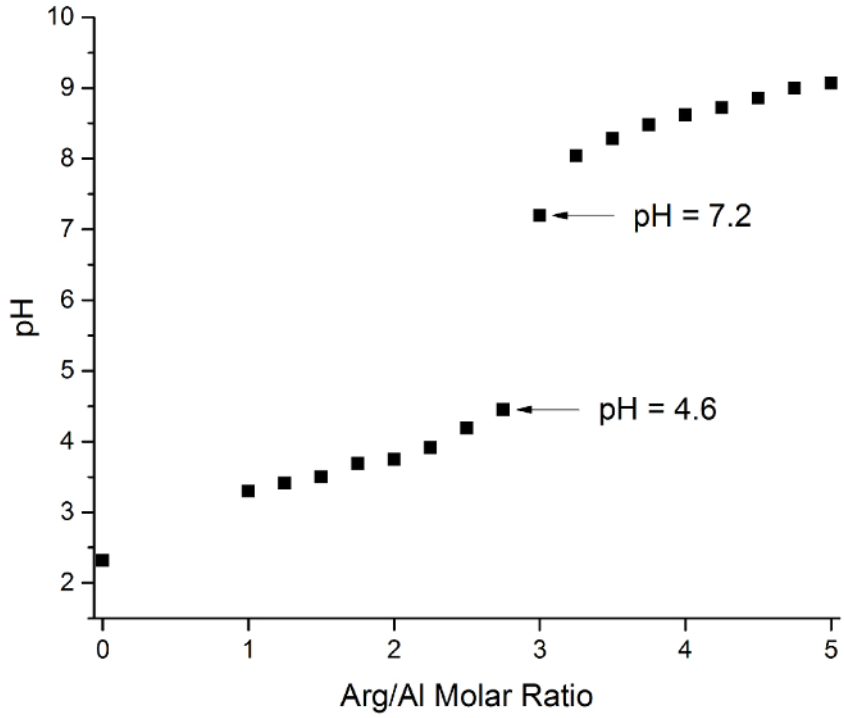


**Figure 5:** Measured pH values at various Arg/Al molar ratios. The arrows point to the samples comprised of Arg/Al ratios of 2.75 and 3.00, which show a drastic increase in pH after the further addition of arginine past the nanogibbsite-containing Arg/Al 2.75 sample. Please click here to view a larger version of this figure.

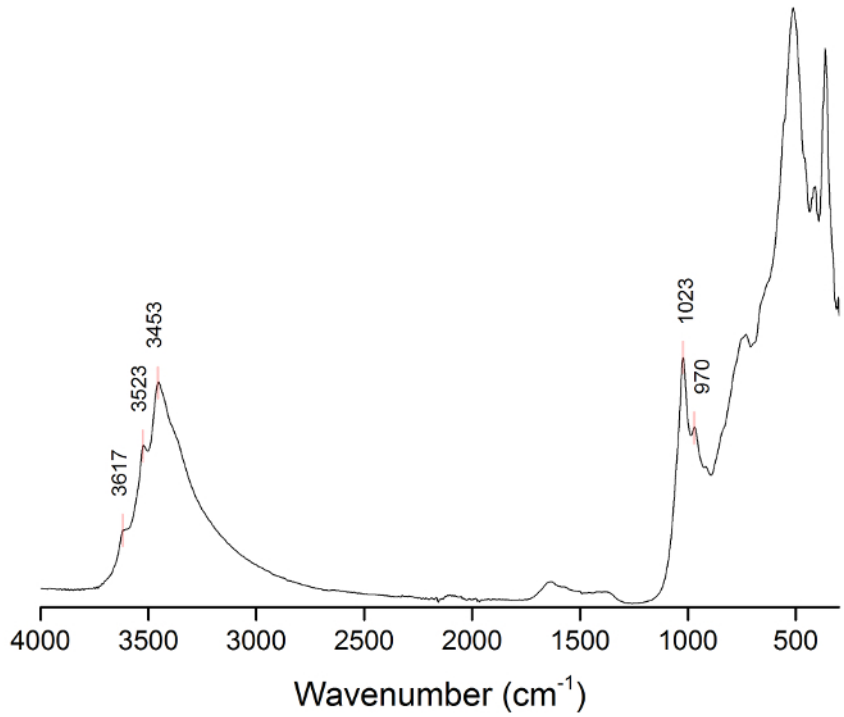


**Figure 6:** FTIR-ATR absorption spectrum of purified $Al(OH)_3$ powder, with characteristic gibbsite vibrations labeled with their wavenumber values. Please click here to view a larger version of this figure.

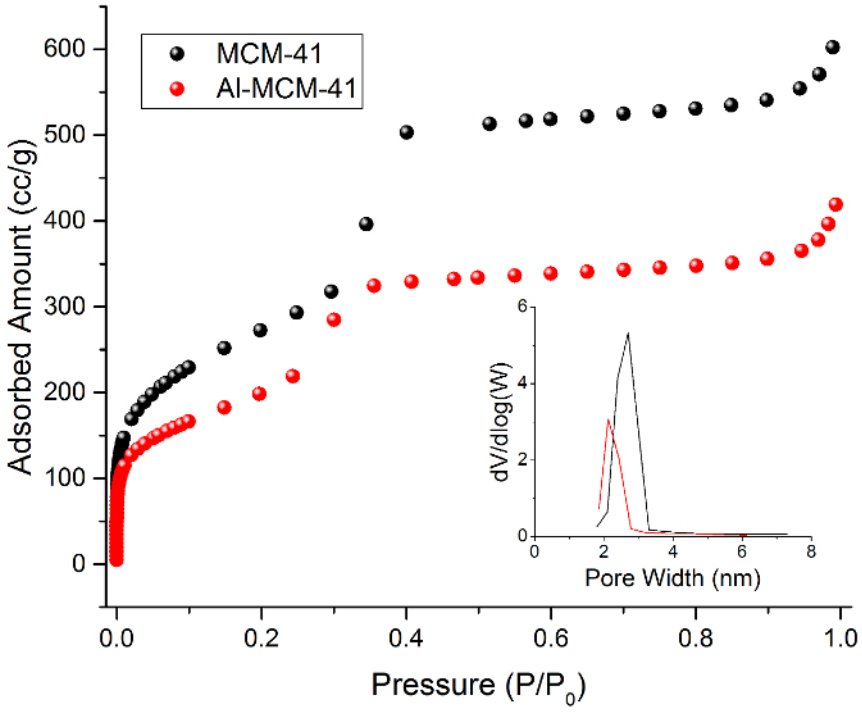


**Figure 7:** $N_2$ sorption isotherms of MCM-41 and Al-MCM-41 obtained via BET method at 77 K. The inset is the corresponding BJH pore size distribution. Please click here to view a larger version of this figure.

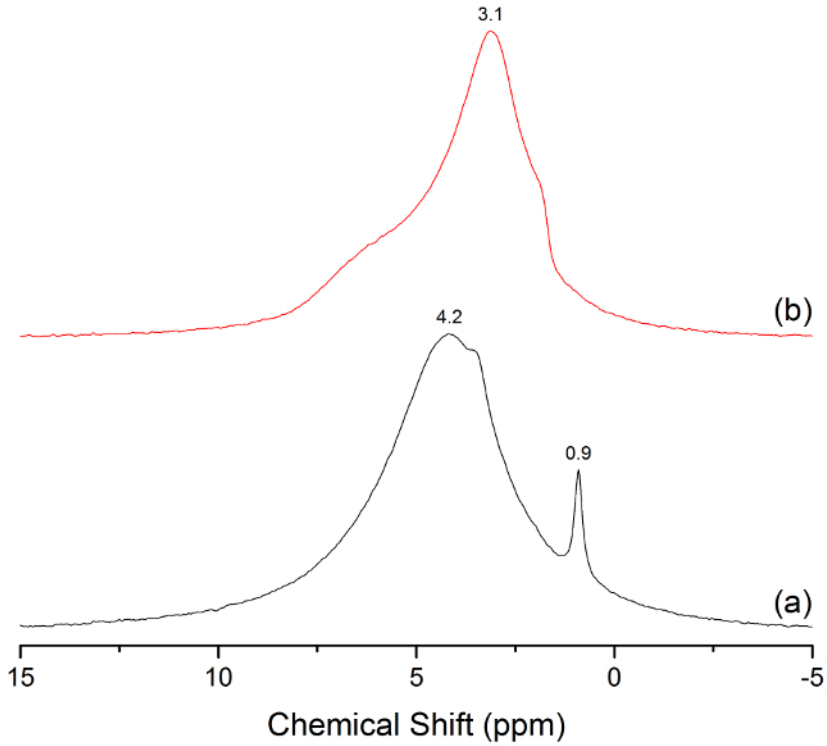


**Figure 8:** $^1H$ MAS NMR spectra of Al-MCM-41 (**a**) and MCM-41 (**b**). The dominant peaks at 0.9, 3.1, and 4.2 ppm are labeled above the respective peak positions. Please click here to view a larger version of this figure.

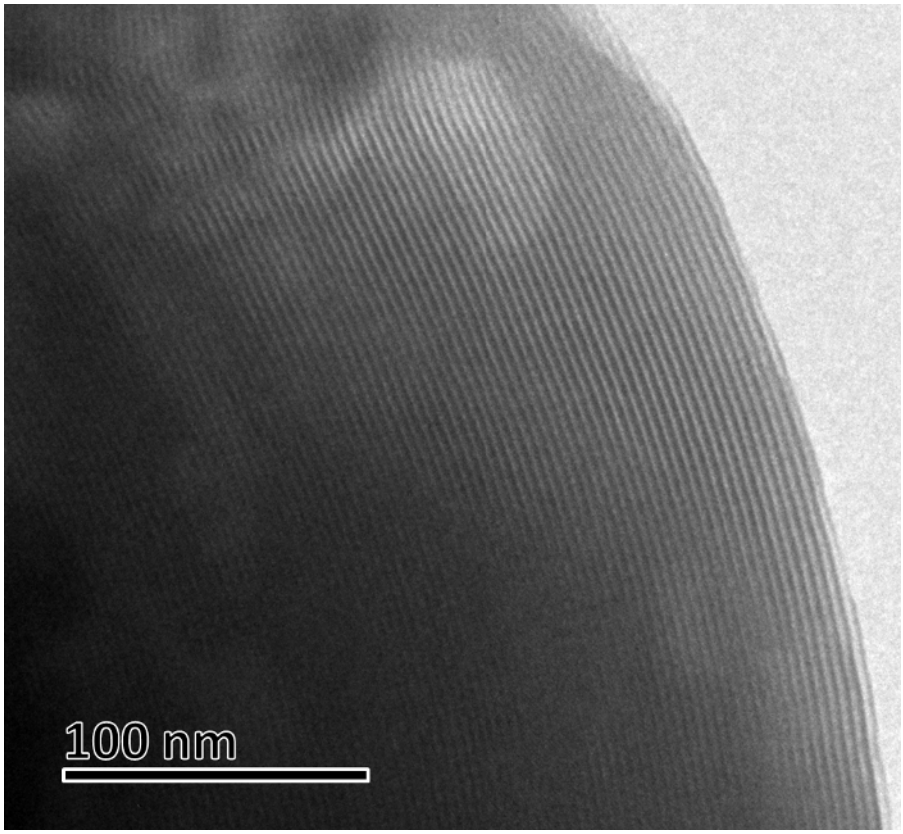


**Figure 9:** TEM micrograph of MCM-41. Scale bar = 100 nm. Please click here to view a larger version of this figure.

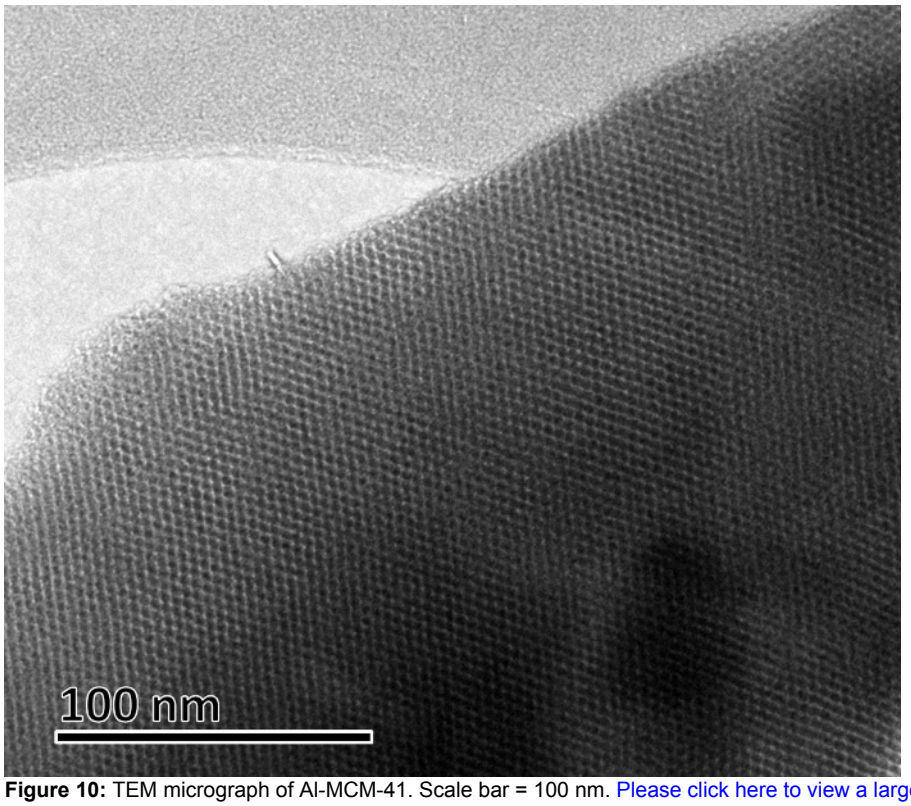


**Figure 10:** TEM micrograph of Al-MCM-41. Scale bar = 100 nm. Please click here to view a larger version of this figure.

## Discussion

The preparation of an aqueous aluminum chloride solution entailed the use of a crystalline hexahydrate salt of aluminum chloride. Although the anhydrous form can also be used, it is not preferred due to its significant hygroscopic properties, which make it difficult to work with and to control the concentration of aluminum. It is noteworthy that aluminum chloride solution should be used within several days of preparation because over time, the $[Al(H_2O)_6]^{3+}$ aqua acid hydrolyzes to yield undesired byproducts that can ultimately reduce the overall yield and purity of the final product. The synthetic methodology described here was conducted with a range of aluminum concentrations (~0.8-3.1 wt% Al). At the higher Al concentrations, the limitation of arginine solubility was reached; therefore, the synthesis could not proceed as intended. On the other hand, the lower concentrations of Al yielded smaller concentrations of nano-$Al(OH)_3$. Previous methodologies incorporated strong bases (*e.g.*, NaOH), the decomposition of molecules to yield a base source (*e.g.*, urea), and ion exchange resin as a mild hydroxide source for hydrolysis.[1,18,19] To the best of our knowledge, the use of organic molecules such as amino acids has not been previously incorporated to hydrolyze aluminum chloride. Furthermore, the synthesis of high-purity $Al(OH)_3$ nanoparticles has not been reported using the hydrolysis of an aluminum chloride pathway.

Purification of the prepared nanogibbsite suspension was successfully conducted using a variety of gel packing amounts, packing morphologies, and flow rates. Due to the fragile plastic connectors on our column, the flow rate limitation was approximately 0.5 mL/min, with a majority of the purifications conducted at 0.2 mL/min. The retention time of nanogibbsite particles ranged based on the flow rate and amount of packing material. It is imperative that the column packing material is allowed to pack slowly, which means adding about 1 in of packing material at a time and flowing water at 0.2 mL/min for approximately 30 min to allow the gel to pack well. Moreover, after adding about half a column-worth of packing material, we allowed 24 h of water to flow through the column, which significantly enhanced the packing efficiency of the column. An initial run was conducted to measure the retention time of the two refractive peaks observed (*i.e.*, nanogibbsite and arginine) on the column. Subsequently, the as-synthesized solution was separated on the column, and the two peaks were collected in 10 or 30 min intervals within the time span of the peaks. It was then necessary to analyze the various vials for aluminum and arginine concentrations to understand the species eluting under the specific peak. Due to the large amount of water flowing through the column, the obtained purified solution was significantly diluted.

For the loading of Al into mesoporous silica material, it is important to activate the material prior to the experiment to remove surface-adsorbed gas and liquid impurities, ensuring maximum loading within the pores. A wide variety of solid porous materials besides silica can be used as supports for the guest nanogibbsite molecules (*e.g.*, mesoporous carbon, mesoporous transitional metal oxides, *etc.*), which can significantly increase the impact of the current synthetic methodology. During the heating process, it is ideal to maintain the temperature and duration to below 80 °C and less than 3-5 days, respectively. Increasing the heating temperature or time can cause the aggregation of nanogibbsite particles and can block pores or coat the surface with aluminum. The developed method achieves a relatively high loading of Al and a concentration of octahedral Al as compared to other methods.

## Disclosures

The authors have nothing to disclose.

## Acknowledgements

The authors extend their appreciation to Dr. Thomas J. Emge and Wei Liu of Rutgers University for their analysis and expertise in small-angle X-ray diffraction and powder X-ray diffraction. Furthermore, the authors acknowledge Hao Wang for his support with the $N_2$ adsorption experiments.

## References

1. Laden, K. Antiperspirants and Deodorants, 2nd ed. *Marcel Dekker, Inc., New York.* (1999).
2. Kumara, C.K., Ng, W.J., Bandara, A., Weerasooriya, R. Nanogibbsite: Synthesis and characterization. *J. Colloid Interface Sci.* **352** (2), 252-258 (2010).
3. Demichelis, R., Noel, Y., Ugliengo, P., Zicovich-Wilson, C.M., Dovesi, R. Physico-Chemical Features of Aluminum Hydroxides As Modeled with the Hybrid B3LYP Functional and Localized Basis Functions. *J.Phys. Chem. C.* **115** (27), 13107-13134 (2011).
4. Elderfield, H., Hem, J.D. The development of crystalline structure in aluminum hydroxide polymorphs on ageing. *Mineral. Mag.* **39**, 89-96 (1973).
5. Wang, S.-L., Johnston, C.T. Assignment of the structural OH stretching bands of gibbsite. *Am. Mineral.* **85**, 739-744 (2000).
6. Balan, E., Lazzer, M., Morin, G., Mauri, F. First-principles study of the OH-stretching modes of gibbsite. *Am. Mineral.* **91** (1), 115-119 (2006).
7. Scherrer, P. Bestimmung der Grosse und der inneren Struktur von Kolloidteilchen mittels Rontgenstrahlen *Gottingen.*, **26**, 98-100 (1918).
8. Langford, J.I., Wilson, A.J.C. Scherrer after sixty years: a survey and some new results in the determination of crystallite size. *J. Appl. Cryst.* **11** (2), 102-113 (1978).
9. Swaddle, T.W., et al. Kinetic Evidence for Five-Coordination in AlOH(aq)2+ Ion. *Science.* **308** (5727), 1450-1453 (2005).
10. Casey, W.H. Large Aqueous Aluminum Hydroxide Molecules. *Chem. Rev.* **106** (1), 1-16 (2006).
11. Lutzenkirchen, J., et al. Adsorption of Al13-Keggin clusters to sapphire c-plane single crystals: Kinetic observations by streaming current measurements. *Appl. Surf. Sci.* **256** (17), 5406-5411 (2010).
12. Mokaya, R., Jones, W. Efficient post-synthesis alumination of MCM-41 using aluminum chlorohydrate containing Al polycations. *J. Mater. Chem.* **9** (2), 555-561 (1999).
13. Brunauer, S., Deming, L.S., Deming, W. E., Teller, E. A theory of the van der Waals adsorption of gases. *J. Am. Chem. Soc.* **62**, 1723-1732 (1940).

 

14. Kresge, C.T., Leonowicz, M.E., Roth, W.J., Vartuli, J.C., Beck, J.S. Ordered mesoporous molecular sieves synthesized by a liquid-crystal template mechanism. *Nature*. **359** (6397), 710-712 (1992).
15. Zeng, Q., Nekvasil, H., Grey, C.P. Proton Environments in Hydrous Aluminosilicate Glasses: A 1H MAS, 1H/27Al, and 1H/23Na TRAPDOR NMR Study. *J. Phys. Chem. B.* **103** (35), 7406-7415 (1999).
16. Kao, H.-M., Grey, C.P. Probing the Bronsted and Lewis acidity of zeolite HY: A 1H/27Al and 15N/27Al TRAPDOOR NMR study of mono-methylamine adsorbed on HY. *J. Phys. Chem.* **100** (12), 5105-5117 (1996).
17. DeCanio, E.C., Edwards, J.C., Bruno, J.W. Solid-state 1H MAS NMR characterization of γ-alumina and modified γ-aluminas. *J. Catal.* **148** (1), 76-83 (1994).
18. Shafran, K.L., Deschaume, O., Perry, C.C. The static anion exchange method for generation of high purity aluminium polyoxocations and monodisperse aluminum hydroxide nanoparticles. *J. Mater. Chem.* **15** (33), 3415-3423 (2005).
19. Vogels, R.J.M.J., Kloprogge, J.T., Geus, J.W. Homogeneous forced hydrolysis of aluminum through the thermal decomposition of urea. *J. Colloid Interface Sci.* **285** (1), 86-93 (2005).

 